ISBN: 978-3-95450-132-8 doi:10.18429/JACoW-IPAC2014-WEPME028

SYSTEMATIC MEASUREMENT OF THE PUMPING CAPABILITIES OF CRYOGENIC SURFACES

F. Chill[#], IAP, Frankfurt am Main, Germany
L. Bozyk, P. Spiller, GSI, Darmstadt, Germany
O. Kester, GSI, Darmstadt, Germany; IAP, Frankfurt am Main, Germany

Abstract

The quality of the beam vacuum is crucial for the stable operation of synchrotrons with high intensity heavy ions. Cryogenic surfaces are capable of pumping residual gases by cryocondensation until the saturated vapor pressure (SVP) is reached. Even at LHe temperatures the SVP of hydrogen is too high. If the surface coverage is sufficiently low, residual gas can also be bound by cryosorption, yielding in acceptable low pressures.

These pumping capabilities can be described by two parameters, both dependent on surface temperature and coverage: The sticking probability (SP), that is the chance of an impinging gas particle to be bound, and the mean sojourn time (MST) of a particle on the surface.

To acquire these parameters, an experimental setup is currently built at GSI. It consists of a cryogenic chamber, cooled by a cold head and a warm part with vacuum diagnostics and gas inlet. It allows monitoring the pumping speed and also the equilibrium pressure of the cryogenic part from which the SP and the MST can be deducted.

The results will be used to further improve the accuracy of the dynamic vacuum simulations in cryogenic areas of particle accelerators.

CONCEPT OF THE MEASUREMENTS

The concept for the measurement of the two mentioned parameters is based on the following formulas, which are also used in the dynamic vacuum simulations [1]:

$$(1)\quad S=\frac{1}{4}\sigma\bar{v}A \qquad (2)\quad N_{ads}=S\frac{p}{k_b T} \qquad (3)\quad N_{des}=\frac{N_{bound}}{\tau}$$

Equation (1) shows, that the SP σ is directly linked to the volume pumping speed S if the size of the cold surface and the temperature of the residual gas is known. This means that it can be measured by a Pneurop Dome like configuration [2] which is made up of two volumes connected by a well defined conductance bezel. Equation (2) describes the number of adsorbed particles per second as a function of pressure and temperature. For the equilibrium case $N_{ads} = N_{des}$ it can be combined with equation (3), which contains the MST τ. A measurement of the isotherms like the one performed by Wallén [3] can be used to determine τ if S is already known by using this combined equation. The isotherm is the particle density in the volume plotted against the surface coverage on the walls in the case of equilibrium for a given temperature.

Based on these considerations, the experimental setup (Fig. 1) was developed to be capable of two different measurements: In the first phase, the residual gas species in question is led into the system through two chambers which are connected by a well defined conductance. This allows the measurement of the pumping speed of the cold surface and also to keep track of the amount of gas which was bound on the cryogenic surface and thereby its coverage. For the second phase the conductance is completely closed to observe the equilibrium pressure of the cold chamber. This yields one point on the isotherm. By sequentially repeating those two phases one can acquire the SP and MST for different surface coverages. With integrated heating wires one can then set different temperatures on the cold surface to measure another isotherm. The target temperature range is 4 K to 40 K.

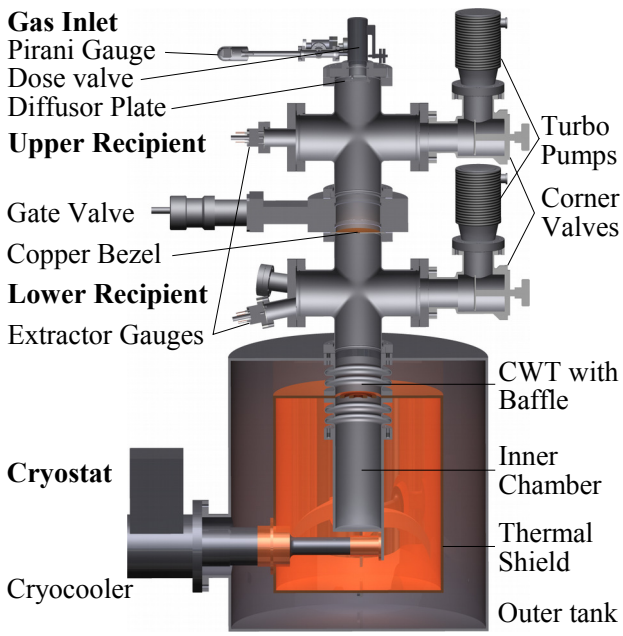

Figure 1: Draft of the measurement setup.

DATA INVERSION WITH MOLFLOW+

As the warm diagnosis part is not a standardized Pneurop Dome, one has to find an individual way of linking the measured pressure ratio to the pumping speed. To achieve this, the tool MolFlow+ [4] has been used to calculate expected pressure ratios for different SP values assigned to the cold surface. Some results of those calculations are shown in Fig. 2. The statistical error of the pressure ratios determined by the Monte Carlo simulations is <0.5% and thereby negligible compared to the errors of the pressure gauges. The course of the curves depends on the geometry of the vacuum system. In this

[#]f.chill@gsi.de

ISBN: 978-3-95450-132-8 doi:10.18429/JACoW-IPAC2014-WEPME028

case, the transmission probability of the baffle in the cold warm transition (cwt) was varied.

The error propagation from the pressures to the resulting SP value is proportional to the slope of the SP over pressure ratio plot (Fig. 2) at each point. This means one can already predict the error of the SP measurements (Fig. 3). For this picture it was pessimistically assumed that the 10% error of the pressures were purely of statistical nature and thus lead to an error of over 14% when building the ratio. To improve this, both gauges have been previously levelled to each other in a single, spherical recipient. Thereby, most of the systematic calibration error will cancel out when building the pressure ratio. The qualitative message of Fig. 3 however is not altered by this: The sweet spot for the SP measurement lays around 0.01, which is the magnitude found by previous research [5]. The accuracy drops drastically towards higher SP. This is due to the fact that almost all particles have multiple contacts with the cold walls before they may find their way back into the warm part, where they can be detected by the gauges. Increasing the transmission of the cwt by decreasing the baffle opacity generally improves the accuracy and expands the effective measuring region. Opening or even removing the baffle might lead to excess heat loads on the inner chamber, which is investigated in the next chapter.

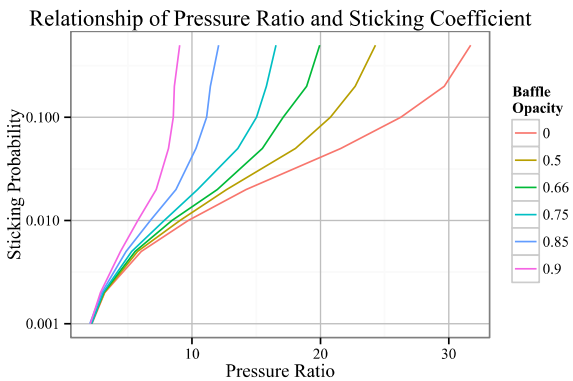

Figure 2: Curves linking possible SP of the cold surface to the measured pressure ratio as calculated by MolFlow+.

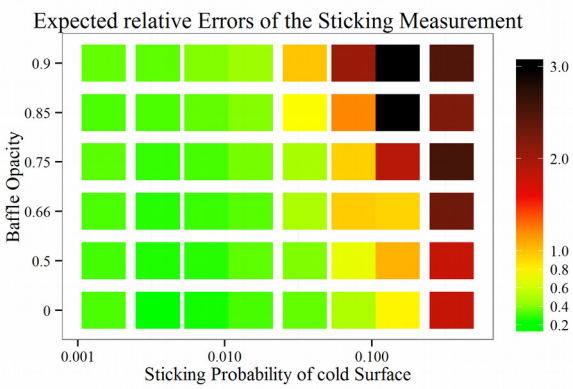

Figure 3: SP around 1% can be determined with the highest accuracy. A high opacity of the baffle lowers the cwt conductance and increases the magnitude of errors.

DEVELOPMENT OF THE CRYOSTAT

The cold stainless steel surface is provided in the form of a small chamber. A homogeneous temperature distribution is ensured by plating it with copper, which has a very high thermal conductivity at cryogenic temperatures. The cryostat (Fig. 1, lower part), that is currently under construction, is tailored around an existing cryocooler. It has a cooling capacity of 1 W at 4 K on its second stage, which is connected to the chamber. This inner chamber is encased by a copper shield which protects it from room temperature heat radiation. The shield is cooled by the first stage of the cryocooler to 40 K. To reach 4 K it is crucial that the heat load on the inner chamber stays below the mentioned cooling capacity.

The overall heat load is made up of three components: Conduction over the bellows and the supports, heat radiation from the shield to the outside of the chamber and heat radiation from the warm part through the cwt. The first one is currently under detailed investigation, but so far it is clear, that it will stay under 0.1 W. The radiation from the thermal shield has been simulated to be only 17 mW even in the worst case of all surfaces having an emissivity of 1. The radiation through the cwt emerged as the most decisive component with a value of ~0.4 W without a baffle. The assumption for this value was an emissivity of 0.5 for the bellows and 0.2 for the electro polished inner surface. Hot filaments burning in the lower warm chamber may increase this value by ~10% per filament. This value strongly depends on whether one assumes diffuse or specular reflections in the warm part.

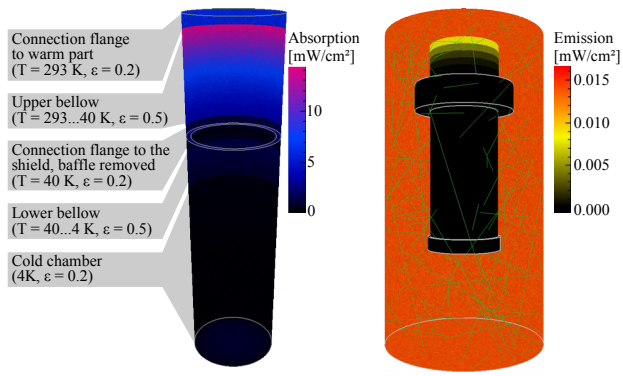

Figure 4: Left: Heat radiation *absorbed* inside the cold chamber. Bellows collect most of the radiation due to higher emissivity. Right: Heat Radiation *emitted* between shield and chamber. Some Monte Carlo radiation beams are shown in green.

The heat radiation was simulated with McCryoT. Fig. 4 shows the geometries used and some resulting textures. The simulations determine the amount of heat absorbed and desorbed from each surface element per second and map those values as color coded pixels onto the geometry. The difference between the two is the net heat flow on each element. This has been summed up over all elements

ISBN: 978-3-95450-132-8 doi:10.18429/JACoW-IPAC2014-WEPME028

belonging to the inner chamber plus the lower half of the lower bellow to get the heat load on the second stage of the cryocooler. As mentioned in the previous section, a high conductance through the cwt leads to greater accuracy in the results, but may cause problems due to greater heat loads.

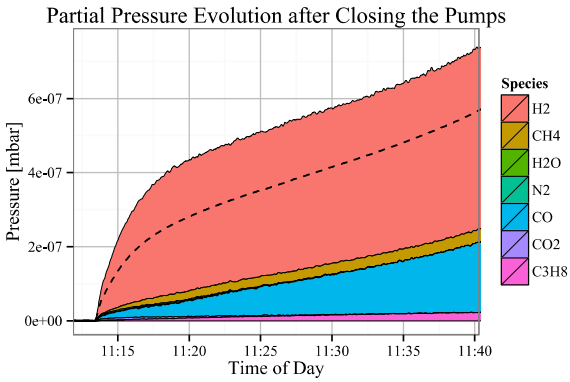

Figure 5: Partial pressures in the lower chamber after closing both corner valves at 11:13. The dashed line shows the nitrogen equivalent pressure displayed by the bottom gauge.

MEASUREMENTS IN THE WARM PART

The warm diagnosis part is already in full operation and has been pumped down and baked out. The goal was to determine the outgassing rate for the two warm chambers. This will pose as background for the cold measurements and has to be considered when calculating the surface coverage. Ultimately an outgassing as low as approximately 2e-9 mbar l / s was reached in the lower chamber. This equals a specific rate of 7e-13 mbar l / s cm². It was measured by two different methods: (1) One of the corner valves in front of the pumps was closed. Then the net gas flow through the conductance equals the outgassing rate in the closed chamber. It can be deducted from the two pressure values. (2) Both corner valves where closed to employ the pressure rise method. The outgassing rate is then the slope of the pressure rise multiplied by the volume of the chambers.

The partial pressure data from one of those pressure rise measurements is shown in Fig. 5. Once the cold part is connected, the gas particles will be pumped by the cold surface instead of building up in the volume. Therefore, this graphic can also be interpreted as the expected background surface coverage over time.

ACKNOWLEDGEMENT

Work is supported by Hic4Fair and BMBF (FKZ: 05P12RDRBK).

REFERENCES

[1] P. Puppel, Dissertation “Umladungsverluste in Schwerionensynchrotrons” (25), Goethe Universität Frankfurt, 2012
[2] K. Jousten, Wutz Handbuch Vakuumtechnik 11. Auflage (764), 2013
[3] E. Wallén, J. Vac. Sci. Technol. A 14(5), 1996
[4] R. Kersevan et al., J. Vac. Sci. Technol. A 27(1017), 2009
[5] V. Baglin et al., Vacuum 67 (421–428), 2002